Environmental Science and Pollution Research (2018) 25:28109–28119
https://doi.org/10.1007/s11356-018-2849-6

RESEARCH ARTICLE

Study on the copper(II)-doped MIL-101(Cr) and its performance in VOCs adsorption

Dongfang Wang[1] · Guiping Wu[2] · Yufeng Zhao[3] · Longzhe Cui[2] · Chul-Ho Shin[4] · Moon-Hee Ryu[1] · Junxiong Cai[5]

Received: 18 May 2018 / Accepted: 25 July 2018 / Published online: 1 August 2018

Abstract

The metal-organic framework (MOF) materials, MIL-101(Cr), and copper-doped MIL-101(Cr) (Cu@MIL-101(Cr)) were prepared through hydrothermal method and were used to remove volatile organic compounds (VOCs) in this study. Morphological characterization demonstrated that MIL-101(Cr) and Cu-3@MIL-101(Cr) were octahedral crystal, with specific surface area of 3367 and 2518 m^2/g, respectively. The results of XRD, TG, and FTIR showed that the copper doping procedure would not alter the skeleton structure, but it would affect the crystallinity and thermal stability of MIL-101(Cr). Besides, MIL-101(Cr) and Cu-3@MIL-101(Cr) displayed good removal efficiencies on benzene sorption, and the maximum sorption capacity was 103.4 and 114.4 mg/g, respectively. In competitive adsorptions, the order of adsorption priority on Cu-3@MIL-101(Cr) was as follows: ethylbenzene > toluene > benzene. Hence, it could be concluded that MIL-101(Cr) and copper-doped MIL-101(Cr) demonstrated good performance in VOCs adsorption and showed a promising potential for large-scale applications in the removal of VOCs.

Keywords MIL-101(Cr) · Cu doping · Hydrothermal method · Volatile organic compounds · Adsorption

Introduction

Porous materials are always hot topics in research due to their special structural properties. In the late twentieth century, a novel kind of material, metal-organic frameworks (MOFs), was firstly reported by Hoskins (Hoskins and Robson 1989) in 1989. This new material was composed of metal ions or metal ion clusters and multi-topic organic ligands (such as ethylenediamine, terephthalic acid, and glycine) and synthesized through the coordination reaction. So that, MOFs have a variety of tunable properties, such as charge, polarity, redox potential, photoactivity, hydrophobicity/hydrophilicity,

Highlights
The adsorption behavior and mechanism of VOCs on MIL-101(Cr) and modified MIL-101(Cr) were investigated.
The copper-doped MIL-101(Cr) showed better adsorption performance of benzene than that of the metal-free MIL-101.
Surface pore diameter and polarity of MIL-101 were important factors affecting the adsorption capacity and affinity for VOCs.

Responsible editor: Tito Roberto Cadaval Jr

Electronic supplementary material The online version of this article (https://doi.org/10.1007/s11356-018-2849-6) contains supplementary material, which is available to authorized users.

✉ Moon-Hee Ryu
ryumoonhee123@gmail.com

✉ Junxiong Cai
cjxhbhjkx@163.com

[1] Division of Biotechnology, College of Environmental and Bioresource Sciences, Chonbuk National University, Iksan 570-752, Republic of Korea

[2] College of Resources and Environmental, South-Central University for Nationalities, Wuhan 430-074, China

[3] Division of Semiconductor and Chemical Engineering, Chonbuk National University, Jeonju 561-756, Republic of Korea

[4] Seohae Environment Science Institute, Jeonju 561-211, Republic of Korea

[5] Hubei Academy of Environmental Sciences, Wuhan 430-072, China

aromatic/lipophilic character, and stereochemistry (Hasan and Jhung 2015; Liu et al. 2014). Besides, one of the most important features is that the synthesis process, which combines merits of numerous metal ions or clusters and organic ligands, can offer copious structural topologies with various porosities (Ahmed and Jhung 2014). Therefore, compared with other porous materials, due to the designability of assembly approach, MOFs have almost unlimited structural models. To date, MOFs have drawn immense attention, and a large number of MOF structures have been created and produced for multifarious applications, such as gas adsorption/storage (Wang et al. 2014a), separation (Li et al. 2015), sensors (Liu et al. 2013), magnetism (Wang et al. 2014b), drug delivery (He et al. 2014), as well as catalysis (Chen et al. 2015). During the many MOFs, MIL-101(Cr), which was designed by Férey et al. (2005) in 2005, has a cubic structure with both great pore volume and uniform pore size. As reported, MIL-101(Cr) has two kinds of quasi spherical cages with the internal diameters of 29 and 34 Å, and accessible through microporous windows of 12 and 16 Å, respectively (Férey et al. 2005). It exhibits good adsorption properties for gas adsorption and storage. Prasanth et al. (2011) studied the adsorption of H_2 on composite materials prepared by MIL-101(Cr) and single wall carbon nanotubes. The results showed that after being combined with single wall carbon nanotubes, the adsorption capacity of H_2 onto MIL-101(Cr) increased from 6.37 to 9.18 wt.% (77 K, 60 bar) and 0.23 to 0.64 wt.% (298 K, 60 bar), respectively. Darunte et al. (2016) prepared an amine-modified MOF material, MIL-101(Cr)-PEI-800, with poly(ethylene imine) (PEI-800) and studied its capturing ability for CO_2 in simulated air. According to the results, the adsorption capacity of MIL-101(Cr)-PEI-800 for CO_2 strongly depended on the amount of amine loading and achieved pseudoequilibrium CO_2 adsorption of 1.35 mmol/g with PEI-800 loading of 1.76 mmol/g MOF.

Recently, air pollutants have attracted wide attention because they are harmful to human health, ecosystems, and atmosphere, especially volatile organic compounds (VOCs). It cannot only cause the greenhouse effect and lead to global warming, but also increase the ozone depletion in the stratosphere and the formation of ozone in the troposphere (Durmusoglu et al. 2009). VOC pollution has gradually become the global environmental issue, which makes many researchers begin to investigate. Considering the structural characteristics, numerous scholars tried to explore the application of MOFs in VOC adsorption. Zhao et al. (2011a) synthesized MIL-101(Cr) through microwave synthesis method, and its uptake of benzene was 16.5 mmol/g at 56 mbar and 288 K. Kun and his co-workers (Yang et al. 2013) reported the MOF-177 which was obtained through solvothermal synthesis at 85 °C for 48 h. The results showed that the adsorption capacity of VOCs on MOF-177 was more than 200.0 mg/g, especially the adsorption capacities of benzene and acetone were as high as 800.0 mg/g and 589.0 mg/g, respectively. Huang et al. (2011) designed a quartz crystal microbalance system to probe the adsorption behavior of MIL-101(Cr) for VOCs and proved that MIL-101(Cr) had high affinity to the VOCs which are composed of heteroatom or aromatic ring and the adsorption capacity could be controlled by adjusting the unsaturated metal sites. Thus, MOFs, with high adsorption ability and affinity to VOCs, are promising materials for the adsorption and storage of VOCs.

To improve the adsorption properties of MOFs, a feasible method is importing unsaturated metal sites into the adsorbent, and there are mainly two approaches to carry it out (Dincă and Long 2008; Zhou et al. 2008). One is that after synthesizing of MOF materials, new unsaturated metal sites can be formed by heating or vacuumizing through dislodging the weakly bound guest water and residual solvent molecules from the metal coordination sites. Llewellyn et al. (2008) had removed the water molecules which were combined with Cr trimers in MIL-101. As a result, the adsorption capacity of CO_2 on MIL-101(Cr) increased from 28.0 to 40.0 mmol/g at 50 bar and 304 K. The second way is inserting metal ions into MOFs by post-synthesized method. Bloch et al. (2010) reported that when copper (II) ions were supported in MOF-253, although the BET surface areas decreased from 2160 to 705 m^2/g, the adsorption percent of CO_2 on MOF-253 increased from 6.2 to 11.7 wt.%. In addition, many researchers had also proved that embedding copper nanoparticles into MOFs materials can enhance gas uptake activity (Wang et al. 2012; Yang 2012). Copper nanoparticles are very useful materials for their remarkable conductivity, good biocompatibility, and economical cost. These properties make them popular and wildly utilized in many applications (Gwilherm et al. 2008; Kidwai et al. 2010; Mitsudome et al. 2008).

The purpose of this work was to explore the adsorption performance of MIL-101(Cr) and copper-doped MIL-101(Cr) on VOCs at atmospheric pressure and room temperature. The MIL-101(Cr) and copper-doped MIL-101(Cr) (Cu@ MIL-101(Cr)) were synthesized and the characterizations were analyzed by X-ray diffraction (XRD), Brunauer–Emmett–Teller (BET) analysis, scanning electron microscopy (SEM), transmission electron microscopy (TEM), X-ray photoelectron spectroscopy (XPS), thermogravimetry (TG), and Fourier transform infrared spectroscopy (FTIR). Then, a suitable experimental scheme, i.e., isotherms, kinetics, and competitive adsorption, was designed and carried out.

Experimental section

Materials

All reagents used in this work were at least analytical grade. Chromium nitrate (99%, $Cr(NO_3)_3 \cdot 9H_2O$), copper nitrate

(99%, $Cu(NO_3)_3{\cdot}3H_2O$)), terephthalic acid (99%, $C_8H_6O_4$), hydrofluoric acid (40 wt.%, HF), dimethylformamide (99.5%, $HCON(CH_3)_2$), methanol (99.9%, CH_3OH), ethanol (99.7%, CH_3CH_2OH), trichloromethane (98%, $CHCl_3$), benzene (99.5%, C_6H_6), toluene (99.5%, C_7H_8), and ethylbenzene (99.5%, C_8H_{10}) were purchased from Sinopharm Chemical Reagent Co., Ltd. (Shanghai, China) and were used as received from vendors without further purification.

Synthesis of MIL-101(Cr) and Cu@MIL-101(Cr)

Hydrothermal method was employed to synthesize MIL-101(Cr) as previous literatures (Férey et al. 2005). In this study, some steps were improved as following: 4.042 g of chromium nitrate (10 mM), 1.342 g of terephthalic acid (8 mM), and 125 μL of hydrofluoric acid (40 wt.%) were added to 70 mL deionized water; then, the mixture was blended by sonication for 30 min and transferred into a teflon-sealed reaction kettle. The reaction kettle was kept in an oven at 210 °C for 8 h. After that, the green samples were obtained by being washed with deionized water and dried in a vacuum oven at 80 °C for 12 h. Afterwards, the dried samples were purified by dimethylformamide (DMF) in Soxhlet extraction system for 3 h. The purification process was repeated thrice. Finally, the resulted crystals were washed three times using chloroform ($CHCl_3$) and then dried in a vacuum oven for 12 h at 80 °C for subsequent experiments.

Synthesis procedures of Cu@MIL-101(Cr) were as follows: 4.042 g of chromium nitrate (10 mM) and various concentration of copper nitrate (0.244 g, 10 wt.%; 0.488 g, 20 wt.%; 0.732 g, 30 wt.%) were added to 70 mL deionized water in a beaker, then 1.342 g of terephthalic acid (8 mM) was added slowly with continuous stirring. The following experimental steps were the same as the synthesis process of MIL-101(Cr) mentioned previously, and the products were marked as Cu-1@MIL-101(Cr), Cu-2@MIL-101(Cr), and Cu-3@MIL-101(Cr), respectively.

Instrumental information

X-ray diffraction (XRD) patterns were measured by X-ray diffractometer (Bruker Advanced D8, Germany), which was operated at 40 kV for Cu Kα (λ = 1.5418 Å) radiation from 3° to 30° (2θ angle range) with a scanning speed of 3°/min. The pore properties were characterized with nitrogen adsorption/desorption at liquid nitrogen temperature (77 K) by using Autosorb-1C-Ms (Quantachrome, USA). The surface morphology and element information were carried out by a scanning electron microscope (SEM, supra 40vp, carl zeiss, Germany) operated at 10.0 kV and a combined WDS/EDS (JEOL, JSM-6000 series WDS/EDS system, Japan), and the transmission electron microscope (TEM, Tecnai G20, FEI, USA) images were taken at 80 kV. X-ray photoelectron spectroscopy (XPS) was conducted on AXIS-NOVA (Kratos Analytical, UK), which used a monochromic Mg Kα X-ray source to determine the atoms on the surface of the samples. All binding energies were corrected based on the neutral C 1s peak at 284.6 eV to remove the surface charging effects. The thermal stability was studied with thermal gravimetric analysis (TGA, TG 209 F3, Netzsch, German) by heating the samples from 30 to 600 °C with a rate of 5 °C/min in nitrogen atmosphere. The FTIR spectrum (Nicolet-6700, Thermo, USA), in the wavenumber range from 4000 to 400 cm^{-1}, was determined with KBr as the standard substance. VOC concentrations were investigated by a gas chromatograph (Shimadzu GC-2010, Japan) equipped with a flame ionization detector.

Adsorption experiments

Adsorption experiments were implemented in a sealed glass vessel with a mini fan. Before experiments, remove the air in the glass vessel as much as possible by using a vacuum pump. After that, a certain amount of VOC solution was added into the glass vessel and insured that the VOC solution was volatilized completely (the concentration of VOCs in the glass vessel kept constant). Then, adsorbents were added into the glass vessel and the concentrations of VOCs were determined by using a GC-FID equipment when the adsorption equilibrium was reached. The adsorption capacity of MOFs for VOCs was calculated by the following equation:

$$q_e = \frac{(c_0 - c_e)V}{m} \quad (1)$$

where q_e is the adsorbed amount of VOCs per gram of adsorbent in equilibrium (mg/g), C_o and C_e are the initial and equilibrium VOC concentrations (mg/m^3), respectively. V is the working volume (L), and m is the dried mass of adsorbent (g).

Effect of adsorbent dosage

A series of adsorption experiments were carried out with different sorbent dosage from 0.01 to 0.04 g/L in the glass vessel which contained 600 mg/m^3 of benzene at room temperature. The concentrations of benzene were determined as mentioned before and the removal rate was studied by Eq. (2):

$$R = \frac{c_o - c_e}{c_o} \times 100\% \quad (2)$$

where R is the removal efficiency of the VOCs on the adsorbent (%), C_o and C_e are the initial and equilibrium VOC concentrations (mg/m^3), respectively.

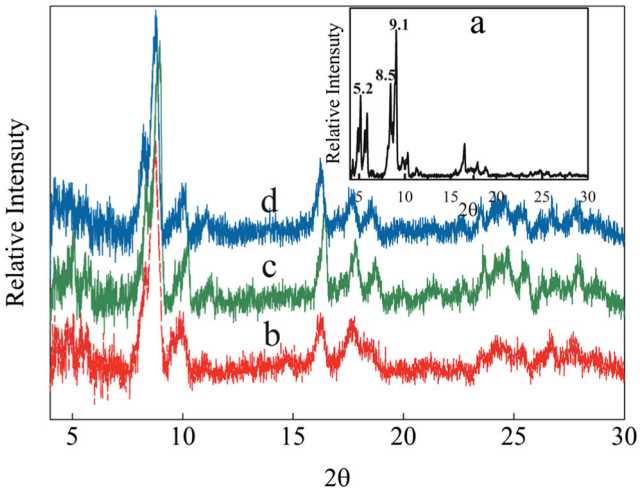

Fig. 1 XRD pattern of various adsorbents (**a** (inset) MIL-101(Cr); **b** Cu-1@MIL-101(Cr); **c** Cu-2@MIL-101(Cr); **d** Cu-3@MIL-101(Cr))

Adsorption kinetics

Kinetic experiments were undertaken as following process: 0.1 g of absorbent was added into the glass vessel in which 600 mg/m^3 of benzene was prepared previously. Samples were collected at a fixed time interval and the residual concentrations were analyzed by GC. The uptake of VOCs at time t, q_t (mg/g), was calculated by the following formula:

$$q_t = \frac{(c_o - c_t)V}{m} \quad (3)$$

where C_t is the concentration of VOCs at any time t (mg/m^3). The kinetic mechanism was evaluated by non-linear pseudo-first-order and pseudo-second-order models.

Adsorption isotherms

Isotherm experiments were conducted with the initial concentrations of VOCs in the range from 0 to 2000 mg/m^3 and adsorbent dosage of 0.02 g/L at room temperature. Similarly, the concentrations of VOCs were determined by GC.

Competitive adsorption study

Competitive adsorption studies were carried out to investigate the adsorption behavior and patterns of Cu-3@MIL-101(Cr) in the mixed compounds, namely benzene, toluene, and ethylbenzene. To explore the impact of concentration on adsorption pattern, concentrations of 500, 1000, and 1500 mg/m^3 were chosen to represent low, medium, and high concentration levels, respectively. Firstly, the same concentration of benzene and ethylbenzene (500, 1000, and 1500 mg/m^3) was prepared in the glass vessel, then 0.02 g/L of Cu-3@MIL-101(Cr) was added. When the reaction reached equilibrium, the adsorption capacities of VOCs were calculated by Eq. (1). After that, competitive adsorptions between benzene and toluene and toluene and ethylbenzene were studied under the initial concentration of 1500 mg/m^3, respectively.

Results and discussion

Characterization

X-ray diffraction analyses

The powder X-ray diffraction patterns of MIL-101(Cr) (Fig. 1a) and Cu@MIL-101(Cr) (Fig. 1b–d) showed that all of the XRD patterns contained the main peaks at 5.2°, 8.5°, and 9.1° which were highly coincident with that of MIL-101(Cr) reported in previous literature (Chen et al. 2013; Férey et al. 2005; Zhao et al. 2011b). It indicated that the products of MIL-101(Cr) were successfully synthesized in this work, and furthermore, copper doping did not change the cage construction of MIL-101(Cr) regardless of the different metal contents (XRD pattern of MIL-101(Cr) prepared by original method was showed in Fig. S1). However, there were some differences in the patterns when the copper was doped into MIL-101(Cr). Especially with the increase of Cu concentration, the XRD patterns showed more impure peaks and lower peak intensity. It implied that copper doping would

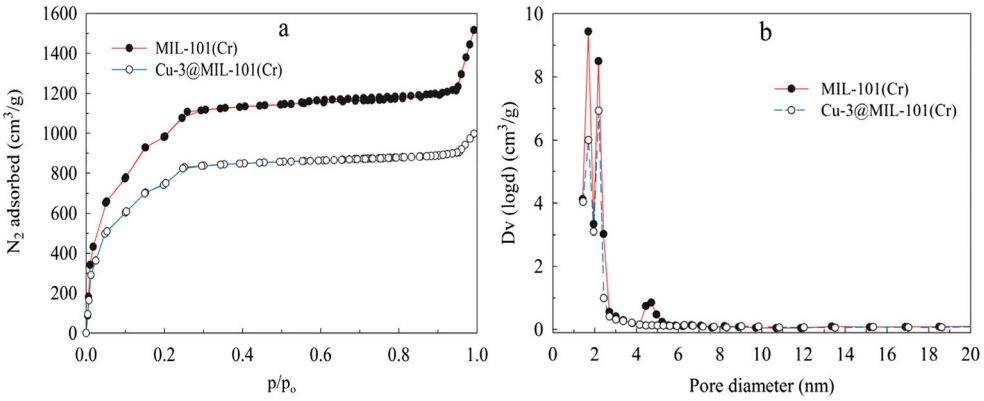

Fig. 2 **a** N_2 adsorption isotherms and **b** pore size distributions (N_2 isotherms were measured at 77 K)

Table 1 Texture properties of materials

Materials	S_{BET} (m^2/g)	Pore volume (cm^3/g)	Reference
MIL-101(Cr)	3367	2.35 (at $p/p_o = 0.99$)	Present work
Cu-3@MIL-101(Cr)	2518	1.55 (at $p/p_o = 0.99$)	Present work
MIL-101(Cr)	4100	2.00	(Férey et al. 2005)
MIL-101(Cr)	2887	1.45	(Prasanth et al. 2011)
MIL-101(Cr)	2800	1.37	(Llewellyn et al. 2008)
MIL-101(Cr)	2014	1.18	(Santiago-Portillo et al. 2015)
MIL-101(Cr)	3060	1.45	(Wickenheisser et al. 2015)

affect the crystallinity of MIL-101(Cr), namely the crystallinity would be decreased with the increased copper concentration (Shen et al. 2015).

Specific surface areas and pore sizes

The nitrogen adsorption and desorption isotherms of MIL-101(Cr) and Cu-3@MIL-101(Cr) (Fig. 2a) both displayed a typical type I profile with secondary uptakes, which demonstrated that two kinds of microporous windows existed in the samples (Férey et al. 2005; Rouquerol et al. 2013). Type I adsorption isotherm usually indicates that the adsorption occurs on the surface of materials or monolayer adsorption happens caused by a strong interaction between the adsorbent and the adsorbate (Kruk and Jaroniec 2001). Moreover, the pore size distributions (Fig. 2b) exhibited that the surface pore diameters were mainly allocated between 1.43 and 2.42 nm; thus, micropores and mesoporous were the major pores in the materials. The structural parameters of the materials prepared in this work and other works are listed in Table 1.

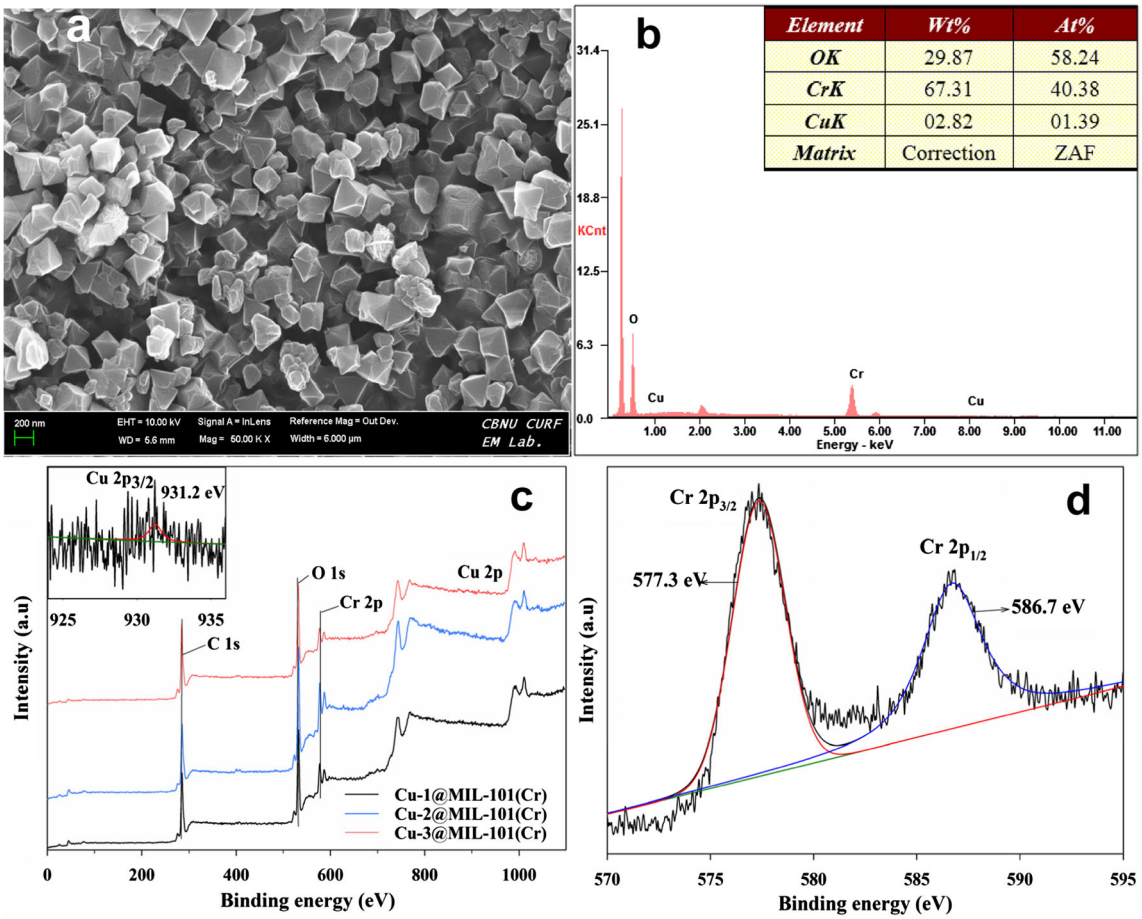

Fig. 3 **a** SEM image of Cu-3@MIL-101. **b** EDX analysis of Cu-3@MIL-101. **c** XPS analysis of Cu@MIL-101 (inset shows the binding energies of Cu). **d** XPS Cr 2p binding energies

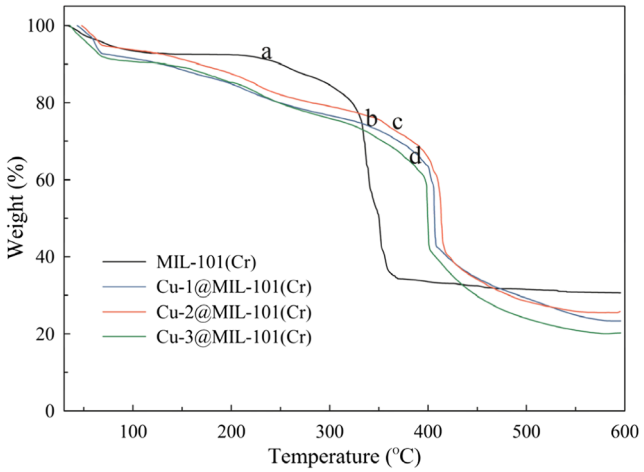

Fig. 4 TG curve of various adsorbents (**a** MIL-101(Cr); **b** Cu-1@MIL-101(Cr); **c** Cu-2@MIL-101(Cr); **d** Cu-3@MIL-101(Cr)

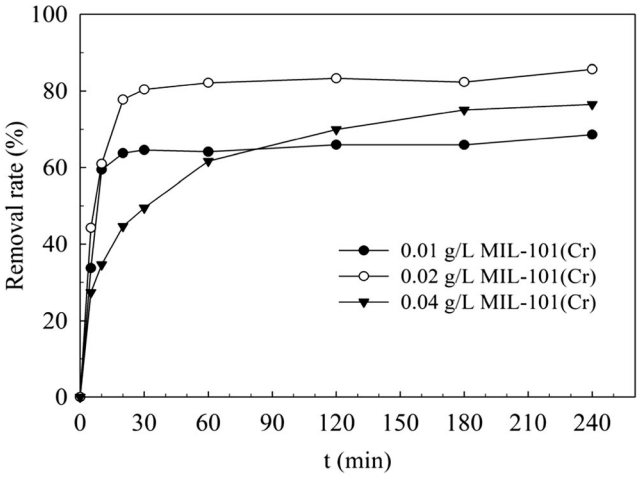

Fig. 6 Effect of sorbent dosage on the removal of benzene using MIL-101 (Cr) (initial concentration: 600 mg/m^3, room temperature)

The data in Table 1 revealed that the MIL-101(Cr) samples synthesized in this work had a large BET-specific surface area (3367 m^2/g) and a high total pore volume (2.35 cm^3/g). But after copper doping, the parameters decreased to 2518 and 1.55 cm^3/g, respectively. The reason for this phenomenon may be that copper ions occupied the interspace of the pores when the doping occurred.

Surface morphology and composition

SEM and EDS images of Cu-3@MIL-101(Cr) are shown in Fig. 3a, b (morphological images of MIL-101(Cr) prepared by original and improved method are shown in Fig. S2), respectively. It could be seen that the Cu-3@MIL-101(Cr) particles were well dispersed, and obvious octahedron structures were clearly displayed as reported previously, with the dimensions of the crystals ranging from 0.2 to 0.4 μm (Zhao et al. 2011a). Besides, the EDS analysis revealed the existence of Cu, which could indicate that the copper was doped into the MIL-101(Cr).

XPS analysis was used to verify the surface element composition of the modified materials (Fig. 3c, d). Figure 3c shows the wide scan XPS spectra of Cu@MIL-101(Cr), and inset of Fig. 3c, d shows the Cu 2p and Cr 2p core-level spectra of Cu-3@MIL-101(Cr), respectively. In the wide spectra, C 1s, O 1s, Cr 2p, and Cu 2p peaks were detected at 284.6, 531.8, 577.3, and 931.2 eV, respectively. Furthermore, due to the binding energy of Cr $2p_{3/2}$ at 577.3 eV (Fig. 3d) and Cu $2p_{3/2}$ at 931.2 eV (inset of Fig. 3c), Cr and Cu in Cu-3@MIL-101(Cr) were identified with 3+ and 1+ states, respectively. The peak intensity of Cu 2p also demonstrated that copper was grafted on the surface of MIL-101(Cr).

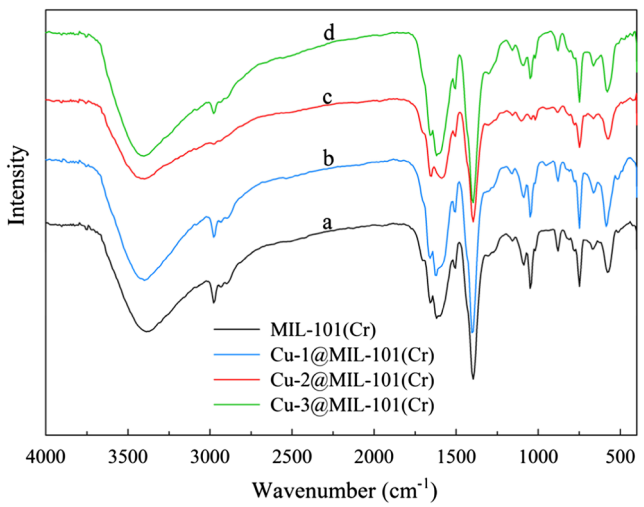

Fig. 5 FTIR spectra of materials (**a** MIL-101(Cr); **b** Cu-1@MIL-101(Cr); **c** Cu-2@MIL-101(Cr); **d** Cu-3@MIL-101(Cr))

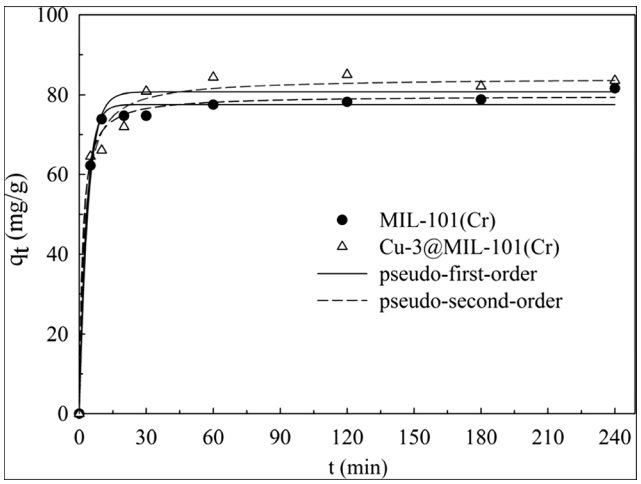

Fig. 7 Adsorption kinetic curves of benzene on MIL-101(Cr) and Cu-3@MIL-101(Cr) (absorbent dosage: 0.1 g, initial concentration: 600 mg/m^3, room temperature)

Table 2 Kinetic parameters of benzene adsorbed by MIL-101(Cr) and Cu-3@MIL-101(Cr), the parentheses are standard deviations

Adsorbent	Pseudo first-order model			Pseudo second-order model		
	q_m (mg/g)	k_1 (min^{-1})	R^2	q_m (mg/g)	k_2(g/(mg · min))	R^2
MIL-101(Cr)	77.56(0.88)	0.32(0.03)	0.994	79.83(0.84)	0.0097(0.0014)	0.996
Cu-3@MIL-101(Cr)	80.70(2.28)	0.26(0.05)	0.962	84.26(1.65)	0.0061(0.0012)	0.987

Thermostability study

As seen from the TG curves, MIL-101(Cr) (Fig. 4a) and Cu@MIL-101(Cr) (Fig. 4b–d) had different thermostability. For MIL-101(Cr), three obvious steps of weight loss were observed. At first, the weight was reduced slightly and slowly in the range of 30.0–214.5 °C, which was caused by the loss of guest water molecules in the large cages. The second step ranged from 214.5 to 324.3 °C and could be due to the loss of guest water molecules from the medium-sized cages. In the third step (above 324.3 °C), the weight was rapidly decreased by nearly 50%, which was attributed to the reduction of OH/F groups caused by the decomposition of the frameworks (Hong et al. 2009). For Cu@MIL-101(Cr), there were also three but different weight loss steps. The weight of materials in the first step (30.0–244.6 °C) reduced about 20%, which would correspond to the loss of weakly bound guest water molecules, gas, and residual solvent from the pores and the Cr trimers (Carson et al. 2013). Compared to MIL-101(Cr), the more weight loss meant the more unsaturated metal sites released on Cu@MIL-101(Cr). So that the adsorption capacity for VOC molecules would be raised because more binding site can be used (Llewellyn et al. 2008). The second and third weight loss steps were situated within the range of 244.6–394.2 °C and above 394.2 °C, respectively.

FTIR spectra

Infrared spectroscopy was applied to explore the functional groups of MIL-101(Cr) and Cu@MIL-101(Cr). It was obviously that the FTIR spectra of the materials obtained in this work (Fig. 5) were similar as that of the MIL-101(Cr) reported in the previous researches (Awadallah-F et al. 2011; Wickenheisser et al. 2015), which confirmed that copper doping did not change the functional groups of MIL-101(Cr). The broad band from 3700 to 3000 cm^{-1} was associated with the O–H stretching vibrations (Zhang et al. 2011). The peak at 2978 cm^{-1} was due to the stretching vibrations of the aliphatic-CH_2. The strong bands at 1612 and 1396 cm^{-1} could be assigned to the vibrational stretching frequencies of O–C–O groups, confirming the presence of dicarboxylate linker in the framework (Jhung et al. 2007; Maksimchuk et al. 2008). And valence vibration bands at 1049 and 748 cm^{-1} revealed the presence of benzene rings (Gu and Yan 2010). The bands at 578 cm^{-1} were most likely to ascribe to in-plane and out-of-plane bending modes of COO– groups (Maksimchuk et al. 2008).

Adsorption studies

Effect of dosage

Removal efficiencies of benzene on MIL-101(Cr) at different adsorbent dose are shown in Fig. 6 (reuse of MIL-101(Cr) on benzene absorption is shown in Fig. S3). It could be seen that with the increasing dosage, the removal rate of benzene increased at first and then decreased. At the dosage of 0.01 and 0.02 g/L, the reactions could reach equilibrium within 15 min, with the removal rate of 68 and 85%, respectively. However, when the dosage increased to 0.04 g/L, the reaction balance time was more than 120 min, as well as the removal rate decreased to 76%. That was because the materials overlapped together which hindered the contact between sorbent and adsorbate. According to this result, the dosage of sorbent in further experiments was 0.02 g/L.

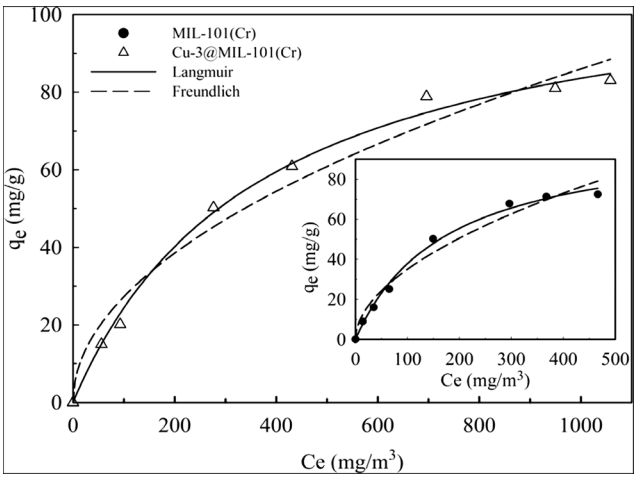

Fig. 8 Adsorption isotherms of benzene on MIL-101(Cr) and Cu-3@MIL-101(Cr) (adsorbent dosage: 0.02 g/L, initial concentration: 0 to 2000 mg/m^3, room temperature)

Table 3 Langmuir and Freundlich isotherm parameters of benzene adsorbed by MIL-101(Cr) and Cu-3@MIL-101(Cr)

Adsorbent	Line type	Langmuir model			Freundlich model		
		q_m (mg/g)	K_L (L/mg)	R^2	K_F (L/g)	n	R^2
MIL-101(Cr)	Non-linear	103.4	0.0058	0.994	3.07	1.89	0.974
	Linear	101.79	0.006	0.992	1.81	1.60	0.983
Cu-3@MIL-101(Cr)	Non-linear	114.4	0.0027	0.996	2.74	2.00	0.974
	Linear	115.4	0.003	0.991	1.39	1.65	0.972

Adsorption kinetics

The effects of reaction time on the adsorption process of benzene by MIL-101(Cr) and Cu@MIL-101(Cr) are shown in Fig. S4. It demonstrated that the adsorption of benzene on MIL-101(Cr) reached equilibrium within 10 min, which was faster than that on Cu-3@MIL-101(Cr). That was because the pore volume in MIL-101(Cr) (2.35 cm^3/g) was larger than that in Cu-3@MIL-101(Cr) (1.55 cm^3/g), and it was easier for benzene molecules to be adsorbed on the pores of MIL-101(Cr). Combined with the analysis of pore size, there were both micropores and mesopores in MIL-101(Cr). However, with the copper doped, the mesopores with diameter range of 2–5 nm almost disappeared and the amount of micropores also decreased in Cu-3@MIL-101(Cr), leading to the relatively slow adsorption rate. Furthermore, the adsorption kinetics (Fig. 7) were investigated by Lagergren pseudo-first-order and pseudo-second-order models. The models were expressed as follows:

$$q_t = q_e\left(1-e^{-k_1 t}\right) \tag{4}$$

$$q_t = \frac{k_2 q_e^2 t}{1 + k_2 q_e t} \tag{5}$$

where q_t (mg/g) and q_e (mg/g) are the adsorption capacity at time t (min) and equilibrium, respectively; k_1 (min^{-1}) and k_2 (g/mg·min) are the kinetic rate constants for the pseudo-first-order and the pseudo-second-order models, respectively. The correlation coefficients (Table 2) for pseudo-second-order model were higher than that for pseudo-first-order model, which meant that chemical process played a crucial role in the adsorption (Lin et al. 2011). Meanwhile, it indicated that the electron transfer, exchange, or sharing were generated and chemical bonds were formed in the adsorption process (Ge et al. 2012).

Adsorption isotherms

The adsorption isotherms were studied at different initial concentrations that ranged from 0 to 2000 mg/m^3. As is well known, the maximum adsorption capacity is an important parameter for sorbents, while Langmuir and Freundlich models are commonly used to calculate it (Freundlich 1906; Langmuir 1918). The non-linear and linear equations of isotherm models were expressed as follows:

$$\text{Langmuir equation}: \quad q_e = \frac{q_m K_L c_e}{1 + K_L c_e} \quad \text{(non-linear)} \tag{6}$$

Table 4 Comparison of VOCs adsorption property on various adsorbents

Adsorbates	Adsorbents	Temperature (°C)	Adsorption capacity	Reference
Benzene	Cu-3@MIL-101(Cr)	25	114.4 mg/g	Present work
Benzene	IRMOF-3	25	56 mg/g	(Britt et al. 2008)
Benzene	IRMOF-62	25	109 mg/g	(Britt et al. 2008)
Benzene	MOF-5	25	2 mg/g	(Britt et al. 2008)
Benzene	MOF-74	25	96 mg/g	(Britt et al. 2008)
Benzene	MOF-199	25	176 mg/g	(Britt et al. 2008)
Benzene	HZSM-5 Zeolite	30	1.9 mmol/g	(Jhung et al. 2007)
Benzene	SBA-15	30	3.0 mmol/g	(Jhung et al. 2007)
Toluene	MIL-101(Cr)	25	0.53 mmol/g	(Huang et al. 2011)
Toluene	Y-Zeolite	20	1.625 mmol/g	(Kim et al. 2007)
Ethylbenzene	MOF-5	150	99 mg/g	(Gu et al. 2009)
Ethylbenzene	MIL-47	130	35 wt.%	(Finsy et al. 2008)

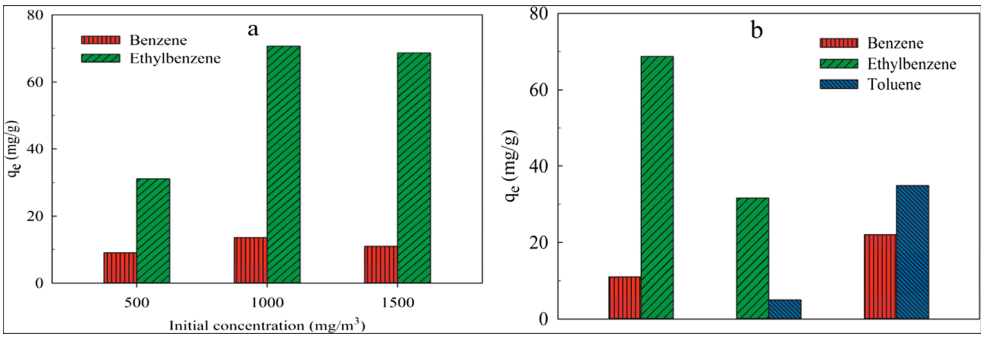

Fig. 9 Competitive adsorptions of VOCs on Cu-3@MIL-101(Cr) (**a** bi-VOCs system, **b** tri-VOCs system)

$$\frac{c_e}{q_e} = \frac{1}{q_m K_L} + \frac{c_e}{q_m} \quad \text{(linear)} \tag{7}$$

$$\text{Freundlich equation}: \quad q_e = K_F c_e^{1/n} \quad \text{(non-linear)} \tag{8}$$

$$\log q_e = \frac{1}{n}\log c_e + \log K_F \quad \text{(linear)} \tag{9}$$

where q_e (mg/g) is the adsorption capacity at equilibrium, C_e (mg/m^3) is the benzene concentration at equilibrium, q_m (mg/g) and K_L are the Langmuir constants, representing the maximum adsorption capacity for the solid phase loading and the energy constant related to the heat of adsorption, respectively. The K_F and $1/n$ are Freundlich constants related to adsorption capacity and intensity of adsorption, respectively. The non-linear adsorption isotherm curves are demonstrated in Fig. 8 (linear fitting curves are displayed in Fig. S5) and the constants are presented in Table 3.

As seen in Table 3, both the non-linear and linear coefficients of determination (R^2) for Langmuir model were more than 0.99 and higher than those for Freundlich model, which suggested that the adsorption of benzene on MIL-101(Cr) and Cu-3@MIL-101(Cr) could be described well by Langmuir model and it was principally monolayer adsorption (Langmuir 1918). In addition, the maximum adsorption capacity of benzene on MIL-101(Cr) and Cu-3@MIL-101(Cr), calculated by non-linear Langmuir model, was 103.4 and 114.4 mg/g, respectively. As mentioned before, copper doping would cause the decrease of specific surface area and pore volume on MIL-101(Cr), resulting in a decrease in adsorption capacity. But at the same time, it also introduced unsaturated metal sites, which would improve the adsorption performance of the materials (Chowdhury et al. 2009). As a consequence, influenced by the two factors, Cu-3@MIL-101(Cr) had a better adsorption property. The adsorption capacities of Cu-3@MIL-101(Cr) in the present work and other adsorbents reported previously are listed in Table 4. Cu-3@MIL-101(Cr) showed a good adsorption capacity for benzene as compared with other adsorbents, suggesting that Cu-3@MIL-101(Cr) was a promising adsorbent in the removal of VOCs.

Competitive adsorption

Competitive adsorption was studied through bi-VOCs and tri-VOCs systems. For bi-VOCs system, adsorptions between benzene and ethylbenzene on Cu-3@MIL-101(Cr) at different concentrations (500, 1000, and 1500 mg/m^3) are exhibited in Fig. 9a. It was obviously that the adsorption capacities of ethylbenzene were much higher than that of benzene and increased with the rising concentration. However, when the concentration was over 1000 mg/m^3, the adsorption capacity remained almost constant. That was because the content of VOCs exceeded the maximum adsorption capacity of adsorbents. Tri-VOCs system for competitive adsorptions among benzene, toluene, and ethylbenzene at the concentration of 1500 mg/m^3 is shown in Fig. 9b. The results illuminated that the priority of adsorption followed this order: ethylbenzene > toluene > benzene, and mutual interference among benzene, toluene, and ethylbenzene, which caused the low adsorption capacity, might exist. It might be ascribed to the functional groups and pore diameters on the surface of materials and the polarity of VOCs (Yaghi et al. 1995). What is more, compared with the only hexatomic ring of benzene, the branched chain in both toluene and ethylbenzene could more easily enter the small pore and combine with MIL-101(Cr) which was of energetic heterogeneity (Huang et al. 2011). Moreover, the longer chain of ethyl, which can get into the pore more deeply, might combine with sorbent more firmly than the short chain of methyl.

Conclusion

In this work, typical metal-organic framework materials of MIL-101(Cr) and Cu@MIL-101(Cr) had been successfully synthesized by improved hydrothermal method. The characterizations showed that the MIL-101(Cr) and Cu@MIL-101(Cr) were octahedral crystal with large specific surface area. Moreover, copper doping did not change its skeleton structure, but there would be some effects on the crystallinity and thermal stability. The VOCs adsorption capacities were investigated by kinetic and isotherm experiments, while Cu-

3@MIL-101(Cr) showed the best performance in absorbing benzene among the four materials with the maximum adsorption capacity of 114.4 mg/g. The Cu@MIL-101(Cr) had better performance in uptake of benzene than the metal-free MIL-101(Cr), probably because it provided more adsorption sites. The competitive adsorption systems of bi-VOCs and tri-VOCs revealed that mutual interference among benzene, toluene, and ethylbenzene might exist in the adsorption process. Furthermore, Cu-3@MIL-101(Cr) preferentially adsorbed ethylbenzene, followed by toluene and finally benzene. In a word, copper doping is an effective modification method to improve the adsorptive property of MIL-101(Cr), and the materials can have good applications in the adsorption, removal, and storage of VOCs and other gases.

References

Ahmed I, Jhung SH (2014) Composites of metal-organic frameworks: preparation and application in adsorption. Mater Today 17:136–146

Awadallah-F A, Elkhatat AM, Al-Muhtaseb SA (2011) Impact of synthesis conditions on meso-and macropore structures of resorcinol-formaldehyde xerogels. J Mater Sci 46:7760–7769

Bloch ED, Britt D, Lee C, Doonan CJ, Uribe-Romo FJ, Furukawa H, Long JR, Yaghi OM (2010) Metal insertion in a microporous metal-organic framework lined with 2,2'-Bipyridine. J Am Chem Soc 132: 14382–14384

Britt D, Tranchemontagne D, Yaghi OM (2008) Metal-organic frameworks with high capacity and selectivity for harmful gases. P Natl Acad Sci USA 105:11623–11627

Carson F, Su J, Plateroprats AE, Wan W, Yun Y, Samain L, Zou X (2013) Framework isomerism in vanadium metal-organic frameworks: MIL-88B(V) and MIL-101(V). Cryst Growth Des 13:5036–5044

Chen H, Chen S, Yuan X, Zhang Y (2013) Facile synthesis of metal-organic framework MIL-101 from 4-NIm-Cr $(NO_3)_3$-H_2 BDC-H_2O. Mater Lett 100:230–232

Chen YZ, Xu Q, Yu SH, Jiang HL (2015) Tiny Pd@co Core-Shell nanoparticles confined inside a metal-organic framework for highly efficient catalysis. Small 11:71-76

Chowdhury P, Bikkina C, Gumma S (2009) Gas adsorption properties of the chromium-based metal organic framework MIL-101. J Phys Chem C 113:6616–6621

Darunte LA, Oetomo AD, Walton KS, Sholl DS, Jones CW (2016) Direct air capture of CO_2 using amine functionalized MIL-101 (Cr). ACS Sustain Chem Eng 4:5761–5768

Dincă M, Long JR (2008) Hydrogen storage in microporous metal-organic frameworks with exposed metal sites. Angew Chem Int Edit 47:6766–6779

Durmusoglu E, Taspinar F, Karademir A (2009) Health risk assessment of BTEX emissions in the landfill environment. J Hazard Mater 176: 870–877

Férey G, Mellot-Draznieks C, Serre C, Millange F, Dutour J, Surblé S, Margiolaki I (2005) A chromium terephthalate-based solid with unusually large pore volumes and surface area. Science 309:2040–2042

Finsy V, Verelst H, Alaerts L, De Vos D, Jacobs PA, Baron GV, Denayer JF (2008) Pore-filling-dependent selectivity effects in the vapor-phase separation of xylene isomers on the metal−organic framework MIL-47. J Am Chem Soc 130:7110–7118

Freundlich H (1906) Over the adsorption in solution. J Phys Chem 57: 1100–1107

Ge F, Li MM, Ye H, Zhao BX (2012) Effective removal of heavy metal ions Cd^{2+}, Zn^{2+}, Pb^{2+}, Cu^{2+} from aqueous solution by polymer-modified magnetic nanoparticles. J Hazard Mater 211:366–372

Gu ZY, Jiang DQ, Wang HF, Cui XY, Yan XP (2009) Adsorption and separation of xylene isomers and ethylbenzene on two Zn−terephthalate metal−organic frameworks. J Phys Chem C 114:311–316

Gu ZY, Yan XP (2010) Metal-organic framework MIL-101 for high-resolution gas-chromatographic separation of xylene isomers and ethylbenzene. Angew Chem Int Edit 49:1477–1480

Gwilherm E, Nicolas B, Mathieu T (2008) Copper-mediated coupling reactions and their applications in natural products and designed biomolecules synthesis. Chem Rev 108:3054–3131

Hasan Z, Jhung SH (2015) Removal of hazardous organics from water using metal-organic frameworks (MOFs): plausible mechanisms for selective adsorptions. J Hazard Mater 283:329–339

He C, Lu K, Liu D, Lin W (2014) Nanoscale metal-organic frameworks for the co-delivery of cisplatin and pooled siRNAs to enhance therapeutic efficacy in drug-resistant ovarian Cancer cells. J Am Chem Soc 136:5181–5184

Hong DY, Hwang YK, Serre C, Férey G, Chang JS (2009) Porous chromium terephthalate MIL-101 with Coordinatively unsaturated sites: surface functionalization, encapsulation, sorption and catalysis. Adv Funct Mater 19:1537–1552

Hoskins BF, Robson R (1989) Infinite polymeric frameworks consisting of three dimensionally linked rod-like segments. J Am Chem Soc 111:5962–5964

Huang CY, Song M, Gu ZY, Wang HF, Yan XP (2011) Probing the adsorption characteristic of metal-organic framework MIL-101 for volatile organic compounds by quartz crystal microbalance. Environ Sci Technol 45:4490–4496

Jhung SH, Lee JH, Yoon JW, Serre C, Férey G, Chang JS (2007) Microwave synthesis of chromium terephthalate MIL-101 and its benzene sorption ability. Adv Mater 19:121–124

Kidwai M, Mishra NK, Bhardwaj S, Jahan A, Kumar A, Mozumdar S (2010) Cu nanoparticles in PEG: a new recyclable catalytic system for N-Arylation of amines with aryl halides. Tetrahedron Lett 2: 1312–1317

Kim JH, Lee SJ, Kim MB, Lee JJ, Lee CH (2007) Sorption equilibrium and thermal regeneration of acetone and toluene vapors on an activated carbon. Ind Eng Chem Res 46:4584–4594

Kruk M, Jaroniec M (2001) Gas adsorption characterization of ordered organic-inorganic nanocomposite materials. Chem Mater 13:3169–3183

Langmuir I (1918) The adsorption of gases on plane surfaces of glass, mica and platinum. J Am Chem Soc 40:1361–1403

Li J, Fu HR, Zhang J, Zheng LS, Tao J (2015) Anionic metal-organic framework for adsorption and separation of light hydrocarbons. Inorg Chem 54:3093–3095

Lin YF, Chen HW, Chien PS, Chiou CS, Liu CC (2011) Application of bifunctional magnetic adsorbent to adsorb metal cations and anionic dyes in aqueous solution. J Hazard Mater 185:1124–1130

Liu D, Lu K, Poon C, Lin W (2013) Metal-organic frameworks as sensory materials and imaging agents. Inorg Chem 53:1916–1924

Liu J, Chen L, Cui H, Zhang J, Zhang L, Su CY (2014) Applications of metal-organic frameworks in heterogeneous supramolecular catalysis. Chem Soc Rev 43:6011–6061

Llewellyn PL, Bourrelly S, Serre C, Vimont A, Daturi M, Hamon L, de Weireld G, Chang JS, Hong DY, Kyu Hwang Y, Hwa Jhung S, Férey (2008) High uptakes of CO_2 and CH_4 in mesoporous metal-organic frameworks MIL-100 and MIL-101. Langmuir 24:7245–7250

Maksimchuk NV, Timofeeva MN, Melgunov MS et al (2008) Heterogeneous selective oxidation catalysts based on coordination polymer MIL-101 and transition metal-substituted polyoxometalates. J Catal 257:315–323

Mitsudome T, Mikami Y, Ebata K, Mizugaki T, Jitsukawa K, Kaneda K (2008) Copper nanoparticles on hydrotalcite as a heterogeneous catalyst for oxidant-free dehydrogenation of alcohols. Chem Commun 39:4804–4806

Prasanth K, Rallapalli P, Raj MC, Bajaj H, Jasra RV (2011) Enhanced hydrogen sorption in single walled carbon nanotube incorporated MIL-101 composite metal-organic framework. Int J Hydrogen Energ 36:7594–7601

Rouquerol J, Rouquerol F, Llewellyn P, Maurin G, Sing KS (2013) Adsorption by powders and porous solids: principles, methodology and applications. Academic press

Santiago-Portillo A, Navalón S, Cirujano FG, Xamena FXL, Alvaro M, Garcia H (2015) MIL-101 as reusable solid catalyst for autoxidation of benzylic hydrocarbons in the absence of additional oxidizing reagents. ACS Catal 5:3216–3224

Shen L, Luo M, Liu Y, Liang R, Jing F, Wu L (2015) Noble-metal-free MoS_2 co-catalyst decorated UiO-66/CdS hybrids for efficient photocatalytic H_2 production. Appl Catal B Environ 166:445–453

Wang D, Zhao T, Cao Y, Yao S, Li G, Huo Q, Liu Y (2014b) High performance gas adsorption and separation of natural gas in two microporous metal-organic frameworks with ternary building units. Chem Commun 50:8648–8650

Wang XJ, Li PZ, Liu L, Zhang Q, Borah P, Wong JD, Chan XX, Rakesh G, Li Y, Zhao Y (2012) Significant gas uptake enhancement by post-exchange of zinc(II) with copper(II) within a metal-organic framework. Chem Commun 48:10286–10288

Wang Y, Xie J, Wu Y, Hu X (2014a) A magnetic metal-organic framework as a new sorbent for solid-phase extraction of copper(II), and its determination by electrothermal AAS. Microchim Acta 181:949–956

Wickenheisser M, Herbst A, Tannert R, Milow B, Janiak C (2015) Hierarchical MOF-xerogel monolith composites from embedding MIL-100 (Fe, Cr) and MIL-101 (Cr) in resorcinol-formaldehyde xerogels for water adsorption applications. Micropor Mesopor Mat 215:143–153

Yaghi OM, Li G, Li H (1995) Selective binding and removal of guests in a microporous metal-organic framework. Nature 378:703–706

Yang H (2012) Doping copper into ZIF-67 for enhancing gas uptake capacity and visible-light-driven photocatalytic degradation of organic dye. J Mater Chem 22:21849–21851

Yang K, Xue F, Sun Q, Yue R, Lin D (2013) Adsorption of volatile organic compounds by metal-organic frameworks MOF-177. J Environ Chem Eng 1:713–718

Zhang Z, Xian S, Xi H, Wang H, Li Z (2011) Improvement of CO_2 adsorption on ZIF-8 crystals modified by enhancing basicity of surface. Chem Eng Sci 66:4878–4888

Zhao Z, Li X, Huang S, Xia Q, Li Z (2011a) Adsorption and diffusion of benzene on chromium-based metal organic framework MIL-101 synthesized by microwave irradiation. Ind Eng Chem Res 50: 2254–2261

Zhao Z, Li X, Li Z (2011b) Adsorption equilibrium and kinetics of p-xylene on chromium-based metal organic framework MIL-101. Chem Eng J 173:150–157

Zhou W, Wu H, Yildirim T (2008) Enhanced H_2 adsorption in isostructural metal-organic frameworks with open metal sites: strong dependence of the binding strength on metal ions. J Am Chem Soc 130:15268–15269